

Magnetic Field Dependence of the Surface Impedance of Superconducting Tin*†

M. SPIEWAK‡

Department of Physics and Institute for the Study of Metals, University of Chicago, Chicago, Illinois

(Received October 27, 1958)

The surface impedance at 1 kMc/sec of superconducting Sn has been investigated as a function of temperature, T , and of static magnetic field, H , both longitudinal and transverse to the rf current. The following unexpected phenomena have been observed. The rf resistance, R , and the reactance, X , may each decrease with increasing H . A decreasing X and an increasing R may coexist. A variation of either the crystalline or static field orientation with respect to the rf magnetic field can change the sign of $[R(H) - R(0)]$ and of $[X(H) - X(0)]$. For $T < 2.0^\circ\text{K}$, both R and X are monotonically increasing functions of H . In this range of T , the approximation of a quadratic dependence for R on longitudinal and transverse H becomes increasingly unsatisfactory with decreasing T . The quadratic coefficient of the variation of X with longitudinal H also decreases with decreasing T , but the corresponding coefficient in transverse H increases, $1.2^\circ\text{K} < T < 2.0^\circ\text{K}$. The relation between these unexpected behaviors and previous experimental and theoretical studies is discussed.

I. INTRODUCTION

THE study of the high-frequency surface impedance¹ provides a powerful tool for investigating the electromagnctic properties of superconductors.^{2,3} In particular, this technique can be applied to obtain detailed information on the behavior of a superconductor in a static magnetic field, H .

The field dependence of the penetration depth, λ , has been discussed theoretically⁴ on the basis of Pippard's measurements as a function of H of the surface impedance, Z , at 9.4 kMc/sec in superconducting Sn.⁵ These experiments have been instrumental both in demonstrating inadequacies of the London theory⁶ and in introducing the concept of coherence in the superconducting electron wave functions. A qualitative explanation of the temperature dependence of the field variation of λ at 9.4 kMc/sec was given by the phenomenological theories of Pippard⁵ and Bardeen.⁶ The unsatisfactory quantitative agreement indicated the desirability of further investigations of the field variation of both R and X .

Results of previous experimental and theoretical studies suggested that both crystalline and static magnetic field orientation relative to the rf fields might be decisive in the determination of $Z(H)$. In the case of Sn, the tetragonal crystal symmetry and the com-

plicated Fermi surface render Z sensitive to crystalline orientation. Crystalline anisotropy effects in tin have been observed with $H=0$ (1) for R in the normal and superconducting states at 9.4 kMc/sec⁷ and 36 kMc/sec⁸; (2) for X in the superconducting state at 9.4 kMc/sec.⁷

Even for crystals with cubic symmetry and a spherical Fermi surface, Ginsburg and Landau⁹ proposed that a marked difference in the observed magnetic field dependence of λ might be expected, depending on whether H was parallel or perpendicular to the high-frequency magnetic field, H_1 . Because of the relationship between Z and λ ,^{5,10} a corresponding magnetic field anisotropy is implied for R and X .

The frequency, $\nu=1$ kMc/sec, was chosen mainly for convenience and for obtaining information on the ν dependence of $Z(H)$. Several factors suggested the desirability of selecting $\nu < 9.4$ kMc/sec. To avoid complications in interpretation arising from the excitation of electrons across the energy gap in a superconductor,¹¹ ν was chosen $\ll kT_c/h$, where T_c =transition temperature= 3.73°K for Sn. In the determination of $\lambda(H)$ from measurements on X , corrections must be applied for the power dissipation by the normal electrons.^{5,10} These corrections depend on a detailed model for a superconductor, but can be made small by choosing ν sufficiently low. Also, by working at $\nu \sim 1$ kMc/sec, it was hoped to obtain information on the relaxation time for equilibrium of the electrons with the radiation field. A lower limit to ν is set by the resonator technique itself.

The measurements were performed on single-crystal wire samples. Provision was made for varying both the magnitude of H and the direction of H relative to

* This research was supported in part by National Science Foundation Grants to the Low Temperature Laboratory of the Institute for the Study of Metals.

† This work is based in part on a thesis submitted in partial fulfillment of the requirements for the degree of Doctor of Philosophy at the University of Chicago.

‡ Standard Oil of Indiana Predoctoral Fellow (1955-1956), Bell Telephone Predoctoral Fellow (1956-1957). Present address: Department of Physics, Cornell University, Ithaca, New York.

¹ A. B. Pippard, *Advances in Electronics and Electron Physics*, edited by L. Marton (Academic Press, Inc., New York, 1954), Vol. 4, p. 1.

² D. Shoenberg, *Superconductivity* (Cambridge University Press, Cambridge, 1952), second edition, Chap. 5.

³ B. Serin, *Handbuch der Physik* (Springer-Verlag, Berlin, 1956), Vol. XV, Chap. 4, p. 241.

⁴ J. Bardeen, *Handbuch der Physik* (Springer-Verlag, Berlin, 1956), Vol. XV, Sec. 30, p. 330.

⁵ A. B. Pippard, Proc. Roy. Soc. (London) **A203**, 210 (1950).

⁶ J. Bardeen, Phys. Rev. **94**, 554 (1954).

⁷ A. B. Pippard, Proc. Roy. Soc. (London) **A203**, 98 (1950).

⁸ E. Fawcett, Proc. Roy. Soc. (London) **A232**, 519 (1955).

⁹ V. L. Ginsburg and L. D. Landau, J. Exptl. Theoret. Phys. (U.S.S.R.) **20**, 1064 (1949). (Summarized in reference 1, pp. 39-40.)

¹⁰ A. B. Pippard, Proc. Roy. Soc. (London) **A191**, 370, 399 (1947).

¹¹ Biondi, Garfunkel, and McCoubrey, Phys. Rev. **108**, 497 (1957).

H_1 . For the microwave resonant cavity used in the experiment, H_1 was excited tangentially to the sample in a plane normal to the wire axis; the principal directions of H were along the sample axis (longitudinal field) or perpendicular to it (transverse field).

The experiment was originally designed to study the field dependence of Z in a transverse H , the direction used by Pippard.⁵ The appearance of an anomalous decrease¹² in X with increasing H suggested variation of the direction of H . The results of the longitudinal-field experiments are emphasized because of the relative simplicity in their interpretation. The transverse- H experiments are treated more qualitatively.

The first part of the paper describes the technique. The second part deals with a presentation of the results on the four experiments: the variation of R and X with longitudinal and transverse H , using as parameters the temperature, T , and the crystalline orientation. The results of the four experiments are then considered as a whole by examining the sources of error and by summarizing the characteristic features of the total problem. The concluding discussion relates the unexpected results to other experimental and theoretical investigations.

II. EXPERIMENTAL METHOD

A. Procedure

The method used to measure the effect of H on the surface impedance of a superconductor as a function of T is similar to the microwave resonance technique introduced by Pippard at 9.4 kMc/sec.^{5,10} The sample constitutes the central conductor of a coaxial resonator. The experimentally observed quantities, the changes in the Q and in the resonant frequency, ν_0 , of the

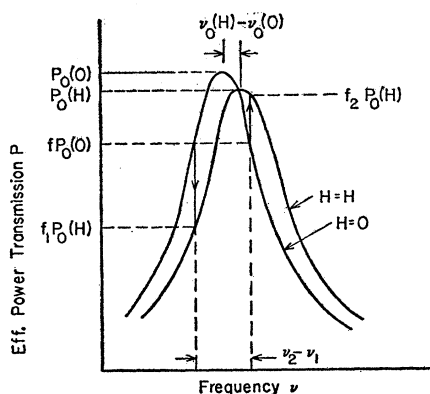


FIG. 1. Comparison between the effective power transmission, $P(\nu, H)$ at $H=0$ and $H=H$, with the maximum transmission, P_0 , occurring at a frequency ν_0 . Observations are made by adjusting ν to ν_1 with $H=0$; $P(\nu_1, 0) = f_1 P_0(0)$, where $0 < f_1 < 1$. (For maximum sensitivity, $f_1 \approx 0.75$.) H is then applied and $f_1 P_0(H)$ is noted. Measurements are repeated at ν_2 on the other side of the resonance. Values of $P_0(0)$, $P_0(H)$, and $(\nu_2 - \nu_1)$ are also recorded. From these data $[\nu_0(H) - \nu_0(0)]$ and $[Q(H) - Q(0)]$ are determined.

¹² M. Spiewak, Phys. Rev. Letters 1, 136 (1958).

resonant cavity, can be directly related to changes in R and X of the sample.¹ In obtaining changes in R and X from the measured quantities, no detailed model for a superconductor is invoked.

The determination of changes in R and X depends on the fact that the effective power transmission, P , of the resonator as a function of frequency, ν , follows a Lorentzian line shape for the sample in either the normal or superconducting state with $H \geq 0$. $P(\nu)$ is obtained from the experimentally observed power transmission after correcting for the variation with ν of the input power to the resonator. The Lorentzian character of the resonance was verified directly at the beginning of every actual experimental run by plotting $P(\nu)$ in detail.

For $H=0$, the temperature variation of R and X at 1 kMc/sec in superconducting Sn is determined from changes in Q and ν_0 between the normal and super-

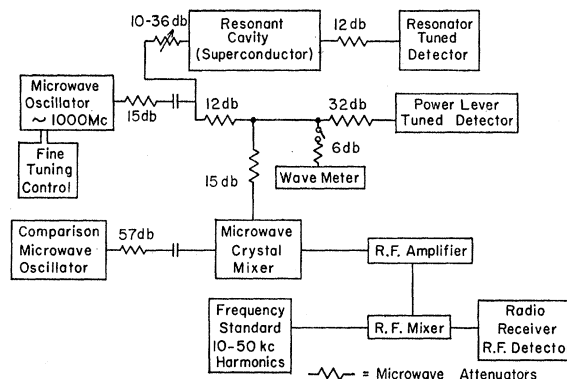


Fig. 2. Schematic diagram of an apparatus for the detection of small changes in the surface impedance of a superconductor. Measurement is made of the power transmitted by the resonator as a function of frequency. The power input to the resonator is monitored at the power-level tuned detector. The two condensers in the diagram pass microwaves but filter lower frequencies.

conducting state.^{1,7,10} Individual resonance curves are studied since the width of the superconducting resonance is generally $\ll [\nu_{0S} - \nu_{0N}]$. The quantity $[\nu_{0S} - \nu_{0N}]$ denotes the change in ν_0 associated with the expulsion of magnetic flux from the skin depth during the transition to the superconducting state.

A determination of the field dependence of Z at constant T requires greater sensitivity, since the effect is small at 1 kMc/sec, the width of the resonance being $\gg [\nu_0(H) - \nu_0(0)]$. By switching H on and off, as shown in Fig. 1, the small changes in Q and ν_0 associated with H are found. This technique, developed by Pippard to study small changes in X ,⁵ minimizes the effect of frequency drift in the oscillator and temperature variation in the resonator. At low T , where the line width becomes narrow, a variation in Z corresponding to $\Delta\lambda \approx 0.2$ A can be resolved. (For Sn, $\lambda \approx 500$ A at $T = 0^\circ\text{K}$.)

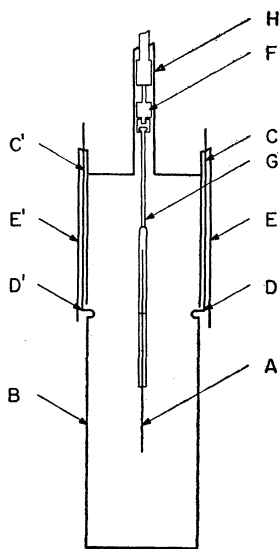
The field variation in X , $[X(H) - X(0)]$, is directly

proportional to the corresponding change in ν_0 . However, to determine changes in R , changes in the "unloaded" Q of the resonator, Q_0 , must be found.¹⁰ Since Q_0 depends on $\xi^{\frac{1}{2}}$ (ξ being the power transmitted by the resonator at resonance), the field variation of ξ must be established also. An interpolation formula is constructed for $\xi(H)$ by determining Q_0 for $H=0$ and for some large H , $H < H_c$, where H_c = critical field. (It is convenient to choose H at $\sim 0.9H_c$ for the case of longitudinal H , and, because of demagnetization effects, just below $0.5H_c$ for transverse H .) Correction for power losses extraneous to the sample need only be applied in the determination of the T dependence of R , since these losses are independent of H and since the H dependence measurements only involve the differences $[R(H) - R(0)]$.

B. Apparatus

Conventional equipment and techniques were generally employed.^{7,10} However, care had to be exercised to attain the required high sensitivity.

FIG. 3. Schematic diagram of the resonator.



Small changes in Z were determined from power and frequency measurements on the apparatus illustrated schematically in Fig. 2. Represented on this diagram are the microwave resonator circuit, the power monitoring circuit, and frequency measuring equipment. The resonant cavity was immersed in a liquid helium bath and surrounded by two magnets which produce H (not shown).

The essential features of the resonator are shown in Fig. 3. Illustrated in Fig. 4(a) are the directions of longitudinal and of transverse H relative to H_1 , the rf magnetic field. The direction of the rf electric current in the sample, j_1 , is also indicated.

The sample, A , a thin single-crystal wire slightly shorter than $\lambda/2$, λ being the wavelength, was made the central conductor of an open circuited coaxial

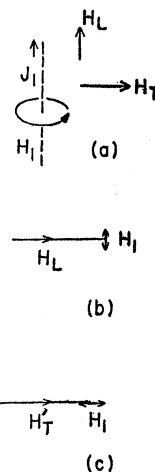


FIG. 4. (a) Directions of the magnetic field, H , and electric current, j , in the resonator relative to the wire direction (dashed line). The subscripts 1, L, T refer to high frequency, static longitudinal, and static transverse, respectively. (b) Field superposition in longitudinal H . (c) Field superposition in transverse H . Demagnetization effects transform the applied field H_T into a local field H_T' directed along H_1 .

resonator. (See Fig. 3.) A specimen diameter of 50–100 μ proved small enough for confining a sufficiently large fraction of the power loss to the sample itself, thereby obtaining the required sensitivity. Surrounding the sample was an oxygen-free, high-conductivity copper tube, B , 10 in. long and 1.5-in. i.d., which served as the outer conductor of the resonator. Power input and output was provided by two identical cupro-nickel coaxial transmission lines, C and C' . The inner conductors, E and E' , terminating in identical beryllium-copper coupling loops, D and D' , short-circuited the transmission lines to B . To minimize reflections produced by coupling to the resonator, a three-meter section of highly attenuating coaxial cable was introduced at the top of the cryostat for both the input and output terminals of the resonator.¹³ Vacuum isolation of the resonator assembly from the helium bath was provided by a copper vacuum jacket. Mechanical isolation was achieved through suitable shock mounts, both internal and external to the helium Dewar vessel.

The sample assembly, F , (see Fig. 3) was inserted into the resonator through a brass tube, H , with the vacuum joint made by a sliding O-ring seal at the top of the apparatus (not shown). Both rotational and linear motion of the sample with respect to the resonator axis was possible. The linear motion permitted variation of ξ , needed to extrapolate $Q(\xi)$ to Q_0 . The rotational motion provided variation of the crystalline orientation relative to transverse H for a given sample.

The sample was cemented with polystyrene cement into two fused quartz rings which served as cross members for a sturdy hairpin-shaped fused quartz bridge, G , readily detachable from the rest of the sample assembly. This design of the quartz bridge eliminated the presence of large quantities of dielectric material in positions of high electric field, thereby minimizing the microwave losses.

¹³ The importance of this precaution had been stressed by T. E. Faber and A. B. Pippard, Proc. Roy. Soc. (London) **A231**, 337 (1955).

TABLE I. Description of the samples.

Sample	Material	Diameter (μ)	α	Orientation		T_c ($^{\circ}$ K)	ν_0 (Mc/sec)
				$\beta(100)$	$\beta(110)$		
Sn1	Vulcan	62	88.5 $^{\circ}$	10 $^{\circ}$	55 $^{\circ}$	3.730	973.4
Sn2	Vulcan	70	29 $^{\circ}$	20 $^{\circ}$	64 $^{\circ}$	3.727	985.1
Sn3	Zone-refined (Tiller)	61	58 $^{\circ}$	10 $^{\circ}$	37 $^{\circ}$	3.727	971.8

Thermal contact between the sample and the helium bath was achieved through exchange gas, using gas pressures low enough to avoid condensation of liquid helium in the resonator. Room-temperature radiation was limited by two copper radiation shields. Thermal stability of $\pm 0.001^{\circ}$ K was required for measuring changes in Z , particularly near T_c . Electronic temperature regulation was used.¹⁴

The microwave oscillator, employing a 2C40 triode, supplied power from 870 to 1150 Mc/sec. Frequency stability of one part in 10^7 could be maintained for several minutes, the time required for measurements at a given H and T . Long-term frequency stability over several days was a few parts in 10^6 . Fine frequency tuning was accomplished by the projection of a fused quartz rod into the oscillator resonant cavity. The rod was driven by a micrometer head calibrated in units of 10^{-5} in. Two quartz rods were employed: one with a resolution of 200 cps over a 3-Mc/sec range, and the other resolved 20 cps in a 300-kc/sec range.

The output from the low-temperature resonator assembly, or alternatively from the power monitoring circuit, was fed to a tuned detector, in which the microwave power was rectified by a 1N21B crystal diode. The resulting dc current was recorded as a deflection on a galvanometer. The sensitivity of the detection scheme was governed by that of the galvanometer, which was 3.3×10^3 mm/ μ a under ordinary operating conditions. The proportionality between the power input to the diode and the rectified current was verified by a detailed determination of $P(\nu)$ for the resonator.

Standard techniques were employed in measuring ν (see Fig. 2). A coaxial wave meter was used for obtaining absolute values of ν to $\pm 0.1\%$. Frequency differences, however, could be detected to a few parts in 10^8 , by mixing two microwave signals to produce an rf voltage, $\nu' < 5$ Mc/sec. This rf signal could then be compared with the 10- and 50-kc/sec harmonics from a frequency standard. In practice, the frequency differences were recorded as divisions on the micrometer head of the fine tuning control, which was calibrated in units of 10 or 50 kc/sec.

The transverse-field magnet was in the form of a pair of 15-in. i.d. Helmholtz coils mounted outside the cryostat, homogeneous to $\pm 0.5\%$ for 18-cm travel along the axis of the resonator. Longitudinal H was generated by a solenoid mounted inside the nitrogen

Dewar vessel of the cryostat assembly, and was homogeneous to $\pm 0.3\%$ over 20-cm travel. By superposition of these fields arbitrary directions of H could be achieved. Measurements to determine the field homogeneity were made at the position of the sample both at room temperature and helium temperatures. Further refinements on field homogeneity were unnecessary since the errors introduced by the rf field were of comparable magnitude. No compensation or correction for the earth's field was made.

C. Samples

The samples were prepared by casting tin into filamentary fused quartz tubes which were later passed through a sharp temperature gradient to produce the single-crystal wires. The fragility of these thin samples necessitated their remaining in the quartz tubes during the course of the experiments. Pippard's work⁷ on larger diameter tin wires (0.25 to 1.0 mm) had shown that specimens surrounded by a quartz sheath yielded the same values for Z as free electropolished samples. Two of the tin samples used in this investigation were prepared from a Vulcan tin ingot (99.98% pure); a third sample was prepared from a higher purity ingot, zone-refined from spec-pure Vulcan tin.¹⁵

The tin wires in the thin quartz sheaths were fabricated in a high-vacuum furnace. The actual casting of the tin was accomplished by forcing a column of the molten metal into a fine capillary quartz tube with clean helium gas. The capillary tubes were drawn from 1-mm bore fused quartz tubes and were cleaned by heat treatment at 500 $^{\circ}$ C in high vacuum.

Since field penetration studies in superconductors emphasize the surface conditions, the estimates of the bulk purity which were made by spectroscopic chemical analysis and low-temperature dc resistivity measurements are of limited interest. These estimates did, however, establish that the bulk purity of the least pure sample was comparable to that used in other high-frequency studies on superconductors.¹⁰ Because of the large ratio of surface area to volume and because of the proximity of the quartz to the tin surface, the surface impurities may exceed the bulk impurities by some undetermined amount. Therefore, no quantitative comparison is possible between the effective purity of the various samples used.

There were several indications that there was no

¹⁴ H. S. Sommers, Jr., Rev. Sci. Instr. **25**, 793 (1954); W. S. Boyle and J. B. Brown, Rev. Sci. Instr. **25**, 359 (1954).

¹⁵ Kindly supplied by Dr. W. A. Tiller, Westinghouse Research Laboratory.

binding between the quartz and Sn surfaces, although small amounts of local adhesion were possibly present. Such adhesion could introduce strains through differential thermal contraction in cooling to helium temperatures. A sensitive test for these strains is the measurement of the field dependence of the surface resistance itself, at low T , since local strains tend to precipitate the formation of regions in the normal state. In order to avoid strains through mounting and cementing the samples in the sample holders, special fixtures were devised. The reliability of results obtained with these samples is assessed in the discussion of errors.

The crystalline orientation of the samples was determined by a standard back reflection Laue method. The angles used to specify the crystallographic orientation of the tetrad axis, α , and of the dyad axis (100), β , relative to the wire axis follow the convention of Fawcett.⁸

A summary is given in Table I of the relevant information on the three tin samples used in this study.

III. THE SURFACE RESISTANCE

A. General Remarks

The variation of R in a superconductor with H is expected to be an even function of H and to be monotonically increasing, slowly for small H and then very rapidly as the normal state is approached. Since, on the basis of the two fluid model of superconductivity, it is the normal electron assembly which contributes to R , then as T is lowered, the magnetic field is expected to be less effective in increasing R .

An unexpected and unexplained effect was reported by Pippard for R in superconducting Sn at 9.4 kMc/sec.⁵ For $3.0^\circ\text{K} \lesssim T \lesssim 3.63^\circ\text{K}$, $R(H)$ was observed to decrease

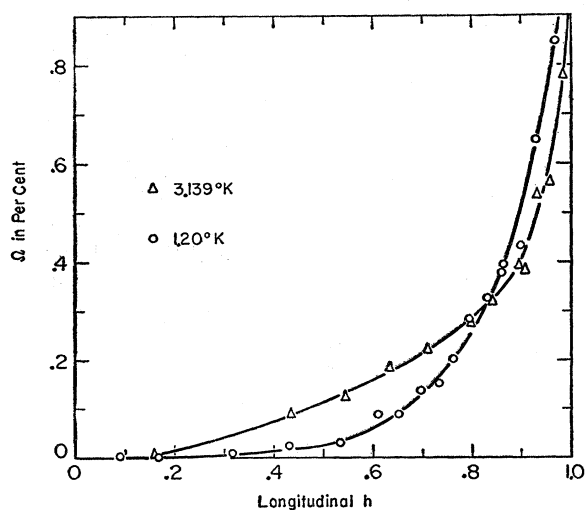


FIG. 5. Relative variation of R at 1 kMc/sec in superconducting Sn (sample Sn1) with longitudinal h . Results for $\Omega(h)$ are similar in the region, $1.2^\circ\text{K} < T < 3.55^\circ\text{K}$. As $h \rightarrow 1$, Ω increases rapidly to $[1 - r(0)]$.

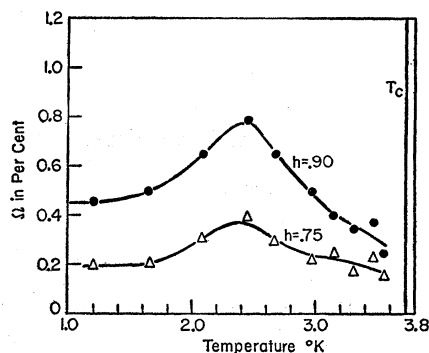


FIG. 6. Relative variation with T of R at 1 kMc/sec in superconducting Sn (Sn1) at constant longitudinal h . The lower curve, $h=0.75$, represents the quadratic field dependence for $1.8^\circ\text{K} < T < 3.55^\circ\text{K}$. Contributions from quartic and higher power terms are important at $h=0.90$ and also for $T < 1.8^\circ\text{K}$ on the curve $h=0.75$. For high T , the T dependence of Ω is governed by the more rapid decrease with T of $r(0)$ than $r(h)$; however, at low T , the T dependence of $r(h)$ supplies the major contribution.

with increasing transverse H . (The transition temperature, $T_e=3.722^\circ\text{K}$.) No detailed discussion of R at 9.4 kMc/sec was given, either as a function of H or T . The appearance¹² at 1 kMc/sec of an anomalous decrease in both R and X with increasing H gave further impetus to a systematic study of $R(H)$.

A discussion of $R(H)$ as a function of T involves the T dependence of $R(H=0)$, previously investigated in superconducting Sn at various frequencies.^{7,8,10,11,16} Just above T_c , the surface resistance in the normal state, R_N , is independent of T . The temperature variation of $r=R/R_N$ at 1 kMc/sec, $H=0$, is similar to that given by Pippard for r at 1.2 kMc/sec.¹⁰ In this range of ν , the scale factor relating r for a given crystalline orientation of Sn is $\nu^{\frac{1}{2}}$.¹⁷ Just below T_c , R falls rapidly with decreasing T . At still lower T , both r and (dr/dT) are small and are monotonically decreasing (e.g., $r \approx 0.01$ at $T \approx 3.0^\circ\text{K}$ at 1 kMc/sec). The measurements indicate that $R \rightarrow 0$ as $T \rightarrow 0$ at 1 kMc/sec. In contrast with the monotonic temperature dependence characteristic of $R(H=0)$ for all crystalline orientations, a complicated variation with T is encountered in the field-dependent term, $[r(H) - r(0)]$.

B. R in Longitudinal Field

The interpretation of the measurements of R in longitudinal H is relatively simple, since H is uniform along the sample (demagnetization effects being absent); therefore, this experiment is presented first.

Typical curves for R on sample Sn1 (see Table I) in the superconducting state are shown at constant T upon variation of longitudinal H (Fig. 5) and at constant reduced magnetic field, $h=H/H_c$, upon variation of T (Fig. 6). For convenience, the field

¹⁶ Blevins, Gordy, and Fairbanks, Phys. Rev. **100**, 1215 (1955); R. E. Glover, III, and M. Tinkham, Phys. Rev. **108**, 243 (1957).

¹⁷ M. D. Sturge, *Conférence de Physique des Basses Températures, Paris, 1955* (Centre National de la Recherche Scientifique and UNESCO, Paris, 1956), p. 563.

variation of R is expressed by plotting the difference $[r(h) - r(0)] \equiv \Omega(h)$ vs h . Thus, in the normal state, $\Omega(h > 1) = [1 - r(0)]$, which differs from unity by $< 1\%$ for $T < 3.0^\circ\text{K}$. Although the functional form of the field plots exhibit only small experimental scatter (see Fig. 5), the measurements are subject to large systematic errors in scale (see Fig. 6), since the determination of the scale factor involves the absolute measurement of a small difference. These errors are accentuated at high T , so that the difference between Ω and $\Omega/[1 - r(0)]$ is less than the experimental error for $1.2^\circ\text{K} < T < 3.55^\circ\text{K}$. In fact, for $3.55^\circ\text{K} < T < T_c$, these errors become so large that this range of T is inaccessible for the experiment summarized by Figs. 5 and 6.

The following statements summarize the behavior of R at 1 kMc/sec for Sn1 as a function of T and of longitudinal H .

- (1) R increases monotonically with increasing H .
- (2) R is only weakly dependent on H . For $h \lesssim 0.9$, $\Omega < 1\%$.
- (3) $\Omega(h)$ is also weakly dependent on T (particularly in comparison with results obtained for other crystalline and magnetic field orientations).
- (4) As $T \rightarrow T_c$, h becomes less effective in increasing R . For $T \geq T_c$, Ω has no meaning.
- (5) As T decreases below 2.0°K , Ω approaches a nonzero value with $(\partial\Omega/\partial T)_h \rightarrow 0$ for $h = 0.75$ and $h = 0.90$.
- (6) For $1.2^\circ\text{K} < T < 3.55^\circ\text{K}$, $\Omega(h)$ can be approximated by a quadratic term $A_L h^2$ for $h < h_{\max}$.

The temperature dependence of the quadratic coefficient, A_L , and of the range of validity of the quadratic approximation, h_{\max} , is shown in Fig. 7. For $2.0^\circ\text{K} < T < 3.4^\circ\text{K}$, A_L is relatively insensitive to variation of T . However, as T decreases from 2.0°K to 1.2°K , A_L is diminished by a factor of ~ 4 . Two alternative curves are suggested by dashes in the region where A_L varies slowly with T , since large errors are involved in the determination of A_L . Reasons for encountering the largest experimental errors in the longitudinal-field experiment on R are considered in the discussion of errors. In the limit $T \rightarrow 0$, a possible extrapolation $A_L \rightarrow 0$ is indicated. The results on Sn1 show the quadratic approximation to become poorer as T decreases from 2.0°K to 1.2°K . Speculations on h_{\max} for $T < 1.2^\circ\text{K}$ are also included in Fig. 7 (dashed curves).

These results on R can be related to the two-fluid model of superconductivity. Power dissipation (or R) is associated with the normal electron assembly. As T decreases below T_c , the normal electron concentration, n_N , decreases and, therefore, so does R . In fact, the theory predicts that $R \rightarrow 0$ as $T \rightarrow 0$ (since $n_N \rightarrow 0$), in agreement with the observations at $\nu = 1$ kMc/sec, $H = 0$. Moreover, for small but finite h , $\Omega(h) \rightarrow 0$ (or at least becomes very small) as $T \rightarrow 0$, as is implied by

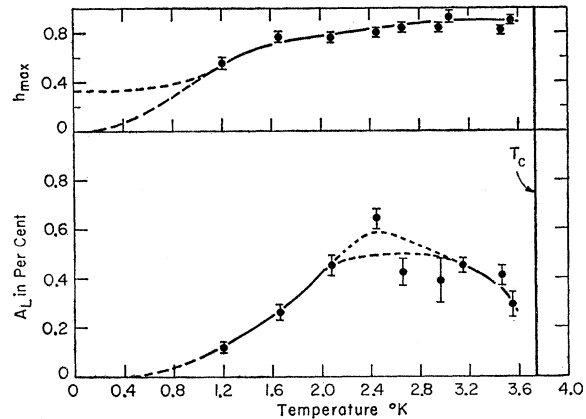


Fig. 7. Lower curve: temperature dependence of the quadratic coefficient, A_L , of Ω at 1 kMc/sec in longitudinal h (see text). Since the errors in A_L for Sn1 are large, two alternate curves (dashes) are suggested for $2.0^\circ\text{K} \lesssim T \lesssim 3.2^\circ\text{K}$, a range of T for which Ω is relatively insensitive to T . In the limit $T \rightarrow 0$, a possible extrapolation $A_L \rightarrow 0$ is indicated. Upper curve: temperature dependence of h_{\max} (see text) associated with A_L . Two possible extrapolations are suggested for h_{\max} as $T \rightarrow 0$.

the extrapolation of $A_L \rightarrow 0$ as $T \rightarrow 0$. The results illustrated in Fig. 7 suggest that a value of $h \gtrsim 0.5$ is needed to rearrange the normal and superconducting electron populations sufficiently to create measurable losses. On the other hand, for Ω to be measurably large at low T , a substantial change in the electronic configuration is required. In fact, for $T \leq 1.2^\circ\text{K}$, a measurably large Ω implies that $[r(h)/r(0)] > 2$.

Because of the decrease in h_{\max} with T for $T < 2.0^\circ\text{K}$, the temperature plot corresponding to $h = 0.75$ in Fig. 6 does not correspond to a quadratic field region in the low- T limit. On the other hand, contributions from quartic and higher power terms are significant for almost the entire range of T in the curve of $h = 0.90$.

The smallness of the field dependence of R in longitudinal h persists upon variation of the crystalline orientation. However, significant differences in the detailed behavior occur from one sample to another. A comparison of $\Omega(h)$ at 1 kMc/sec is shown in Fig. 8 for three Sn samples (crystalline orientations given in Table I) with $T \approx 3.55^\circ\text{K}$, or reduced temperature $t = 0.950 \pm 0.001$. For both Sn1 and Sn2 a monotonic increase in R with h is observed and the field plots are quadratic for $h < 0.85$. The quadratic coefficient, A_L , depends on T , on crystalline orientation, and also, perhaps, on sample purity.

In contrast with the results on Sn1 and Sn2, an unexpected decrease in R with increasing h occurs for Sn3. This decrease in R will be referred to as *anomalous*. Even in the case of Sn3, the field plot for Ω is quadratic for $h < 0.4$, with the quadratic coefficient $(A_L)_3 < 0$. In magnitude, $(A_L)_1 < |(A_L)_3| < (A_L)_2$. Since $\Omega(h > 1) = [1 - r(0)] > 0$, the anomalous decrease in R is accompanied by a minimum in Ω . Thus, in the range of h for which the minimum in Ω occurs, a dependence on

h more complicated than quadratic prevails. The observation of an anomalous decrease in R is considered one of the important results of this investigation.

The crystalline anisotropy effects observed for finite H may be related to anisotropy effects reported for $R(H=0)$ at 9.4 kMc/sec⁷ and at 36 kMc/sec⁸ in normal and superconducting Sn. The variation of the surface conductance, Σ , in normal Sn is related to changes in the curvature of the Fermi surface. Values of Σ at 36 kMc/sec for the orientations of Sn1, Sn2, and Sn3 are 78, 64, and 53 ohm⁻¹, respectively.⁸ The corresponding values for $R(H=0)$ at 9.4 kMc/sec in superconducting Sn are ≈ 12.5 , 13.5, and 18.0 (arbitrary units), respectively. It is, perhaps, not surprising that $\Omega(h)$ at 1 kMc/sec shows more similarity between Sn1 and Sn2 than between Sn1 and Sn3. It is not clear why $(A_L)_3 < 0$ or why $(A_L)_2 > (A_L)_1$ rather than $(A_L)_1 > (A_L)_2$. Because of differences in sample preparation between Sn1, Sn2, and Sn3 (see Table I), some of the apparent orientation effects may be connected with differences in the bulk purity of the samples. Until experimental data on other crystalline orientations are available, and until the effect of crystalline purity on Ω is determined the detailed features of the field dependence of R will be obscure.

C. R in Transverse Field

Several factors complicate the transverse-field experiments to make comparison with the longitudinal-field case difficult. These complications are connected with the demagnetization effects and with the superposition of dc and rf magnetic fields. Nevertheless, the measurements on the variation of R with transverse H are valuable. A qualitative comparison between R in longitudinal and transverse H for the relatively simple crystalline orientation of Sn1 implies that Ω is more strongly dependent on the direction of H than is expected solely on the basis of demagnetization and field superposition effects. Since the transverse- H experiment is complex, this discussion aims to emphasize general characteristics. The more complicated problem of an arbitrarily directed H is not presented here.

Because of demagnetization effects, the observed R and Ω in a transverse external field H represent an average over a range of local fields with magnitudes between 0 and $2H$ and directed along H_1 . (These averages are designated by \bar{R} and Ω_{Av} .) Although, in principle, a quantity Ω' , associated with a unique value of transverse H , can be computed from a knowledge of the angular dependence of Ω_{Av} , the process is laborious and has not been carried out for the general case. Such a computation is practicable only if it is possible to treat Ω_{Av} as independent of sample rotation about the resonator axis. Preliminary measurements on sample rotation cast some doubt on the validity of this approximation. However, this approximation is useful for

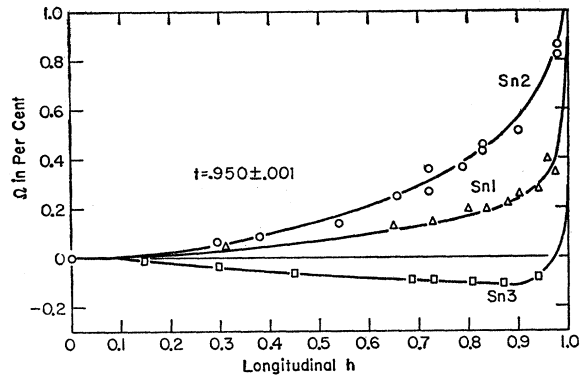


FIG. 8. Relative variation of R at 1 kMc/sec with longitudinal h for three Sn samples (crystalline orientations given in Table I). The anomalous effect in R corresponds to $\Omega < 0$. The relative magnitude and sign of Ω for these samples depends on the reduced temperature, t .

obtaining qualitative information. In particular, for a quadratic dependence of Ω_{Av} on applied H , a short calculation gives $[\Omega'(H)/\Omega_{Av}(H)] = \frac{1}{2}$. It should be noted that since H_1 is excited tangentially to the sample surface, no demagnetization effects are present.

Differences in the dynamic superposition of H_1 on longitudinal and transverse H [see Figs. 4(b) and 4(c)] cause Ω' and Ω to be nonequivalent quantities. The determination of the relation between Ω' and Ω is complicated by crystalline anisotropy effects and by relaxation of the electrons in the rf field. By using a specific model for a superconductor in a magnetic field, an estimate for (Ω'/Ω) can be obtained. (See Sec. VI.)

In Fig. 9, Ω_{Av} at 1 kMc/sec is shown as a function of transverse h for Sn1, $h < 0.6$. At higher h , hysteresis effects associated with the intermediate state occur. The thinness of the wire samples inhibits the formation of the intermediate state for $0.5 \leq h \leq 0.7$, a result also found by Pippard.⁵ In Fig. 10 the corresponding temperature variation of Ω_{Av} at constant external transverse h is illustrated.

The significant differences between the field variation of R in longitudinal and transverse h are summarized by the following points.

- (1) For a given crystalline orientation, Ω may change its *sign*, magnitude and functional form as H changes from longitudinal to transverse.
- (2) A stronger field dependence generally occurs in transverse H . (For example, note the difference in scale between Fig. 5 and Fig. 9.) In particular, the anomalous decrease in R tends to be about one order of magnitude greater than in longitudinal h .
- (3) In contrast with the monotonic field variation in longitudinal h , two mechanisms are operative in transverse h . One, strongly temperature-dependent and dominant at high T , causes R to decrease with increasing h ; the other, prevailing at low T , causes R to increase and has relatively weak temperature dependence.

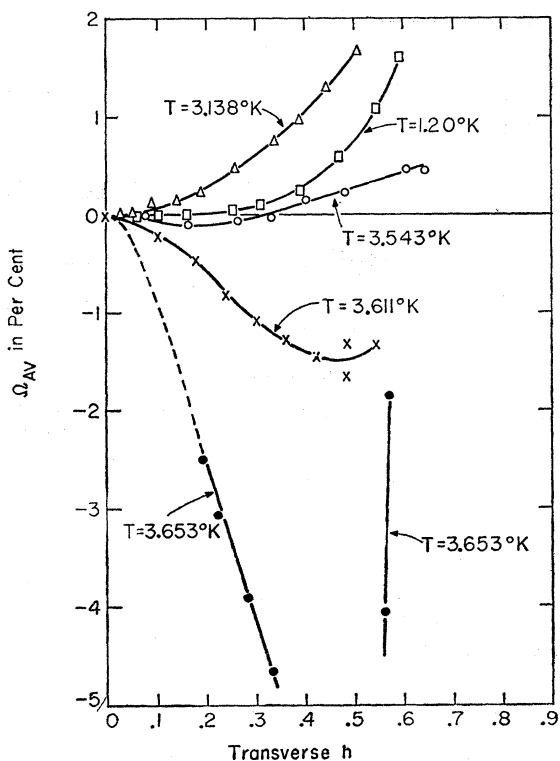


FIG. 9. Relative variation of \bar{R} at 1 kMc/sec in superconducting Sn (Sn1) with transverse h . The anomalous behavior in R (i.e., $\Omega_{AV} < 0$) is characterized by a relatively strong variation of Ω_{AV} with h and T , as is seen in the curves for $T = 3.653^\circ\text{K}$, 3.611°K , 3.543°K . Since $\Omega_{AV} \rightarrow [1 - r(0)]$ as $h \rightarrow 1$, the anomalous behavior in R must give a minimum in Ω_{AV} . At $T = 3.653^\circ\text{K}$, $(\Omega_{AV})_{\min} = -7.7\%$.

Evidence for the existence of these mechanisms comes from the minima appearing in the field plots of Fig. 9. As T decreases, these minima diminish in magnitude and occur at lower values of h . (This discussion is also pertinent to Sn3 in longitudinal h .)

(4) The functional form of Ω_{AV} for Sn1 is more complicated in transverse than in longitudinal h . In particular, for $3.35^\circ\text{K} \lesssim T < T_c$, the anomalous behavior in R is present. The field plots are quadratic for small h , with A_T , the quadratic coefficient, being < 0 ; but, as the minimum in $\Omega_{AV}(h)$ is approached, the field dependence becomes more complicated. For $2.0^\circ\text{K} \lesssim T \lesssim 3.35^\circ\text{K}$, the quadratic approximation is applicable for $h_{\max} \approx 0.5$; and A_T is essentially independent of T for $2.5^\circ\text{K} \lesssim T \lesssim 3.35^\circ\text{K}$. As T decreases below 2.0°K , the quadratic approximation becomes increasingly unsatisfactory with quartic and higher power terms dominating. In fact, the decrease of A_T and of h_{\max} with decreasing T in the low-temperature limit is more pronounced than for the corresponding quantities in longitudinal H . The effect of quartic and higher power terms is emphasized in Ω_{AV} by the strong contribution from small regions in local fields near $2H$.

(5) A strong T dependence for Ω_{AV} in transverse H is associated with the anomalous decrease in R . An

almost vertical slope is encountered in the temperature plots of Fig. 10 for $3.5^\circ\text{K} < T < T_c$.

To isolate the two mechanisms which are operative on R for Sn1 in transverse H , a plot is presented in Fig. 11 of the T dependence of the quadratic coefficient of Ω' , A_T' , at 1 kMc/sec. The branch $A_T' < 0$ illustrates the strong temperature dependence of the anomalous effect in R , while the branch $A_T' > 0$ shows comparatively weak dependence on T . The region of validity of the quadratic approximation for Ω' is shown by the two branches of h_{\max} on the upper curve. The effect of crystalline anisotropy associated with the rotation of the sample about the axis of the resonator has been neglected in the determination of Ω' from Ω_{AV} . A comparison of Fig. 7 with Fig. 11 emphasizes the differences between longitudinal and transverse H with regard to the magnitude of the field dependence of R and to the appearance of the anomalous behavior in R . (For example, note the difference in scale between Fig. 7 and Fig. 11.) However, for the branch of the curves, $A_T' > 0$, both A_L and A_T' are roughly independent of T for $2.5^\circ\text{K} \lesssim T \lesssim 3.3^\circ\text{K}$ and decline with decreasing T for $T < 2.0^\circ\text{K}$. These similarities are qualitative only, since in the temperature-independent region, $(A_T'/A_L) \approx 6.7 \pm 0.9$ while at $T = 1.2^\circ\text{K}$, $(A_T'/A_L) \approx 2$. The extrapolation $A_T' \rightarrow 0$ as $T \rightarrow 0$ is also suggested, with A_T' diminishing more rapidly than A_L as T decreases below 2.0°K .

In transverse, as in longitudinal H , the variation of crystalline orientation gives rise to significant differences in the detailed behavior of $R(h)$. A comparison of Ω_{AV} in transverse H is made in Fig. 12 for Sn1, Sn2, and

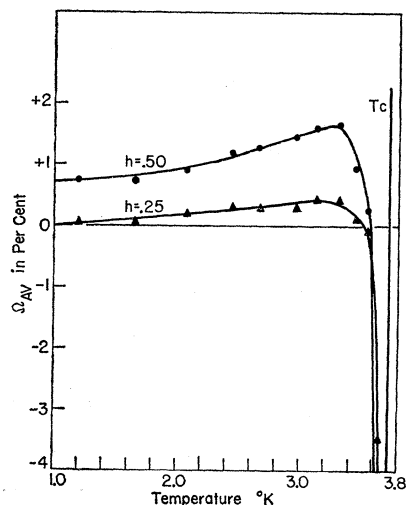


FIG. 10. Relative variation with T of \bar{R} at 1 kMc/sec in superconducting Sn (Sn1) at constant transverse h . The curve, $h = 0.25$, represents the quadratic field dependence for $1.7^\circ\text{K} \lesssim T \lesssim 3.4^\circ\text{K}$. Outside this range of T , higher powers in h are important. The curve $h = 0.50$ represents the quadratic h dependence for $2.2^\circ\text{K} \lesssim T \lesssim 3.2^\circ\text{K}$ and nonquadratic behavior for other T . The strong T dependence of the anomalous effect in R is seen for $3.4^\circ\text{K} \lesssim T < T_c$.

Sn3, $t=0.951\pm 0.001$. For all three samples an anomalous decrease in R is exhibited. These curves are not intended necessarily to imply that all orientations yield $\Omega_{AV} < 0$ in transverse H . Preliminary results on an indium sample, $\alpha=0.5^\circ$, β unspecified, show no anomalous effect in transverse H , although results on another indium sample ($\alpha=88^\circ$, $\beta=26^\circ$) do show this effect. That Ω_{AV} tends to be most negative for Sn3 and most positive for Sn2 is compatible with the results for longitudinal H shown in Fig. 8.

IV. THE SURFACE REACTANCE, X

A. General Remarks

By analogy with metals in the normal state whether described by the theory of the classical or the anomalous skin effect, the variations of R and of X in a superconductor with an external parameter (such as H) are expected to be related to each other. Physically, the electromagnetic energy stored in the surface layer of a metal depends on the dissipation mechanisms characterizing that material. That the field variation of R and of X in a superconductor can be very different at given ν and T is a surprising result.

The variation of X in a superconductor with H is expected to be an even function of H , and to increase monotonically with H , slowly for small H and then rapidly as the normal state is approached. Prior to the present study, information on the T dependence of the field variation of X , $[X(H) - X(0)]$, was limited to observations by Pippard at 9.4 kMc/sec in transverse H . It was found that $X(H) > X(0)$ and that $[X(H) - X(0)]$ does not vanish as $T \rightarrow 0$.⁵

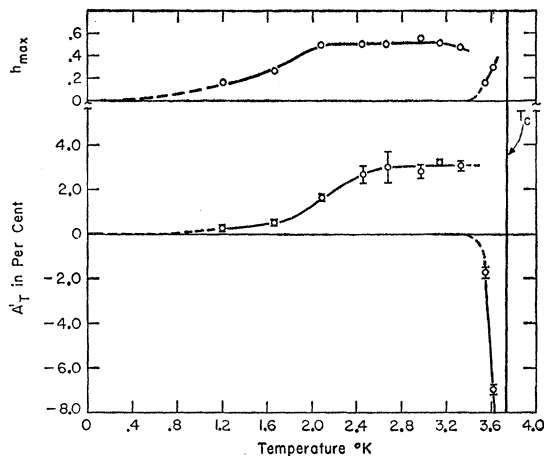


FIG. 11. Lower curve: temperature dependence of the quadratic coefficient, A_T' , of Ω' at 1 kMc/sec in transverse h (see text). Different T dependences characterize the two branches of A_T' ; branch $A_T' < 0$ corresponds to the anomalous decrease in R with h and $A_T' > 0$ to increasing R . The possible extrapolation of $A_T' \rightarrow 0$ as $T \rightarrow 0$ is indicated by the dashed curve. Upper curve: T dependence of h_{max} associated with the two branches of A_T' . The extrapolation of $h_{max} \rightarrow 0$ as $T \rightarrow 0$ is suggested by the dashed curve.

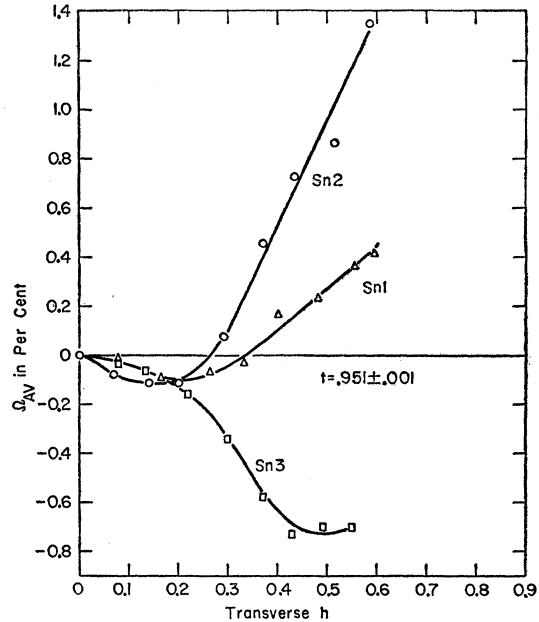


FIG. 12. Relative variation of \bar{R} at 1 kMc/sec with transverse h for three Sn samples (crystalline orientations given in Table I). The anomalous decrease in R differs in detail for these three samples.

This observed behavior at low T is in conflict with the London theory which assumes that the superconducting electron wave functions are independent of H , so that as $T \rightarrow 0$ and $n_N \rightarrow 0$, the electromagnetic properties of the superconductor cannot depend on H . A modified two-fluid model has been presented by Bardeen^{4,6} in which the superconducting electron wave functions are permitted a perturbation in H . Nonzero values for $[X(H) - X(0)]$ are then possible for $T=0$. A second-order perturbation calculation gives a quadratic field dependence of X and of λ which can be fitted qualitatively to Pippard's results at low T .^{5,6} Measurements of the field dependence of X at 1 kMc/sec yield unexpected behaviors regarding variation both with T and with H .

As in the case of R , studies of $X(H)$ involve the T dependence of $X(H=0)$. Investigations at 1.2 kMc/sec¹⁰ and at 9.4 kMc/sec⁷ show, in agreement with the two-fluid model, that $X \propto (1-t^4)^{-1/2}$ for the reduced temperature, t , sufficiently small so that dissipative mechanisms for the normal electron assembly can be neglected. (For example, at 1 kMc/sec this relation would apply for $t < 0.9$.) A more complicated T dependence characterizes the field variation of X , $[X(H) - X(0)]$.

The resonance technique which is used here to study $X(H=0)$ determines directly only changes in X between the superconducting state ($H=0$) and the normal state (H slightly greater than H_c). Denote these changes in X by $\Delta X \equiv [X(0, T) - X(H > H_c, T)] \leq 0$. Since X in the normal state, X_N , is closely temperature independent for $T < T_c$, measurement of the T dependence of ΔX yields both X_N and the T variation of $X(H=0)$.

The results for the field variation of X are conveniently presented by plotting $\Xi \equiv [X(h) - X(0)]/\Delta X$ vs h . In the normal state $\Xi = -1$. The expected increase in X with H yields $\Xi < 0$, while the anomalous decrease in X is represented by $\Xi > 0$.¹² Instead of Ξ , variables referring only to the superconducting state could have been used. Because of the complexity of the observed field variation of X , there is some advantage to presenting the data in a form closest to the experimental observations.

B. X in Longitudinal Field

Results for the temperature dependence of Ξ at 1 kMc/sec in constant longitudinal h are presented for Sn1 in Fig. 13. The corresponding field plots for Ξ at constant T have been presented previously.¹² A comparison between the field dependence of R and of X for a relatively simple crystal orientation (Sn1) can be made using these results on $X(h)$ and the corresponding curves for $R(h)$ in longitudinal h . (See Fig. 5 and Fig. 6.)

The characteristic qualitative behaviors (1-6) described for R at 1 kMc/sec in longitudinal H apply also to X for Sn1 in the superconducting state (with suitable transcription of $R \rightarrow X$). Certain differences, however, appear, particularly in the functional form of Ξ as compared with that of Ω for $T < 2.0^\circ\text{K}$.

For a wide range of T , the variation of Ξ with longitudinal h can be approximated by a term $-B_L h^2$ for $h < h_{\text{max}}$. The temperature dependence of the quadratic coefficient, B_L , and of the range of validity, h_{max} , is illustrated for Sn1 in Fig. 14. Whereas A_L falls by a factor ~ 4 between 2.0°K and 1.2°K , B_L decreases only by $\sim 35\%$ in that temperature range. Also, the departures from the quadratic field dependence at low

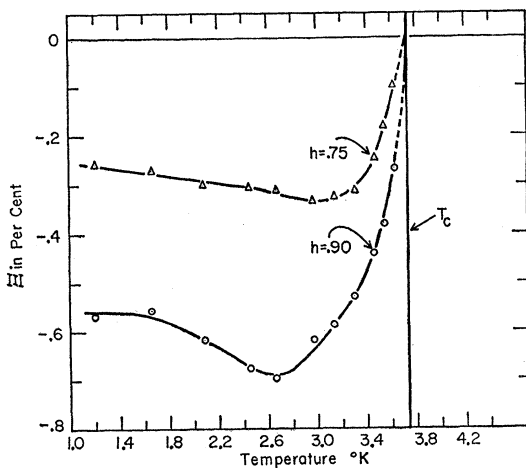


FIG. 13. Relative variation with T of X at 1 kMc/sec in superconducting Sn (Sn1) at constant longitudinal h . For $T \geq 1.6^\circ\text{K}$, the curve $h=0.75$ represents the quadratic field dependence. Contributions from higher power terms are emphasized at lower T and in the curve $h=0.90$. The dashes suggest the decreasing effect of h on X in the limit $T \rightarrow T_c$.

T are less pronounced in Ξ than in Ω (see curves of h_{max} vs T in Figs. 7 and 14). The measurements indicate that at $T=1.2^\circ\text{K}$, $(\partial B_L/\partial T)_h > 0$ and probably also $(\partial^2 B_L/\partial T^2)_h > 0$. On the other hand, the third law of thermodynamics requires that $(\partial B_L/\partial T)_h \rightarrow 0$ as $T \rightarrow 0$. Thus, important information is contained in the inaccessible temperature range, $0^\circ\text{K} < T < 1.2^\circ\text{K}$. The suggested extrapolations of B_L to $T=0^\circ\text{K}$ (see Fig. 14) show that it would not be inconsistent with the measurements to have $B_L \rightarrow 0$ as $T \rightarrow 0$ and to have a quartic field dependence of X (or λ) near $T=0^\circ\text{K}$. Although the available information is at present insufficient to determine the generality of the results of Fig. 14 for other crystalline orientations, it is significant that for at least one sample there are departures from the simple quadratic approximation used in previous studies.⁴⁻⁶ It should be emphasized that negligible experimental error is introduced in the

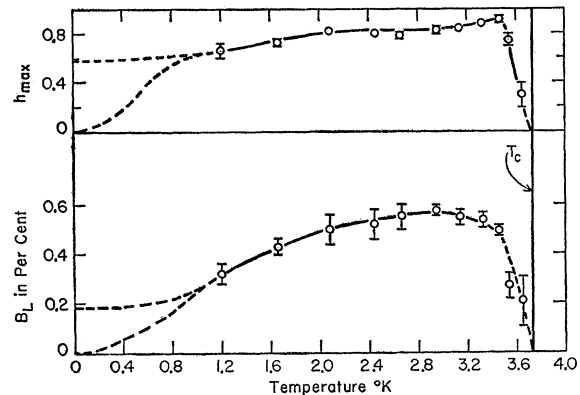


FIG. 14. Lower curve: temperature dependence of the quadratic coefficient, B_L , of $-X$ at 1 kMc/sec in longitudinal h . In the limit $T \rightarrow T_c$, the decreasing effect of h on X is indicated. In the limit $T \rightarrow 0$, extrapolations of B_L to zero and nonzero values are presented. Upper curve: T dependence of h_{max} associated with B_L . Two possible extrapolations are suggested for h_{max} as $T \rightarrow 0$.

determination of the scale factor of Ξ , in contrast with Ω .

Another difference between $\Omega(h)$ and $\Xi(h)$ is related to the temperature at which $(\Omega)_{\text{max}}$ and $(\Xi)_{\text{min}}$ occur (see Fig. 6 and Fig. 13). $(\Xi)_{\text{min}}$ generally tends to be at higher T than does $(\Omega)_{\text{max}}$ with the temperature difference depending on h . (For example, $\Delta T \sim 0.2^\circ\text{K}$ for $h=0.90$ while $\Delta T \sim 0.6^\circ\text{K}$ for $h=0.75$.) However, in both cases the extrema are shallow and broad.

The very large slope of Ξ as $T \rightarrow T_c$ indicates that the temperature dependence of X is stronger than the field dependence in this limit. If $[X(h, T) - X(0, T)] \propto (T - T_c)^n$ and $\Delta X \propto (T - T_c)^m$, then an infinite slope for Ξ as $T \rightarrow T_c$ would imply that $0 < (n - m) < 1$.

The effect of crystalline orientation on Ξ in longitudinal H is illustrated in Fig. 15 at $t=0.950 \pm 0.001$. The corresponding curves for Ω are found in Fig. 8. The monotonic increase in X with h , representable by a quadratic term, occurs for both Sn1 and Sn2. How-

ever, a stronger variation of Ξ with h is found for Sn1 than for Sn2 in contrast with the behavior of Ω shown in Fig. 8. This result indicates that the quantitative correlation between $R(h)$ and $X(h)$ may be sensitive to crystalline orientation or perhaps to sample purity. For Sn3, the anomalous decrease in both R and X occurs with increasing longitudinal h . The behaviors of R and X in Sn3 also have other characteristics in common. Corresponding to the Ω_{\min} , a maximum is found for Ξ with both extrema at $h \sim 0.85$. A quadratic field dependence satisfactorily describes both anomalous behaviors for small h . However, as T is lowered below $\sim 3.3^\circ\text{K}$, the anomalous decrease in X is accompanied by an increase in R [or more generally $(\partial R/\partial H)_T$ and $(\partial X/\partial H)_T$ have opposite signs.] This unexpected effect is discussed further in connection with the transverse-field experiments which emphasize this uncorrelated behavior.

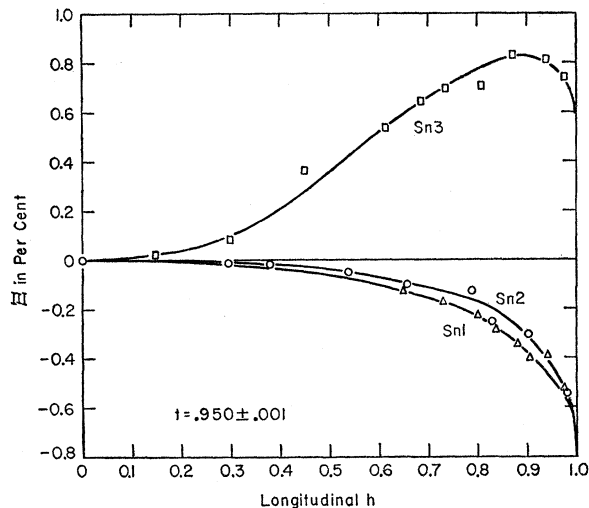


FIG. 15. Relative variation of X at 1 kMc/sec with longitudinal h for three Sn samples (crystalline orientations given in Table I). The anomalous effect in X corresponds to $\Xi > 0$. The relative sign and magnitude of Ξ for these samples depend on the reduced temperature, t .

C. X in Transverse H

Significant differences also exist in $X(H)$ for Sn1 depending on the relative directions between H and the rf field, H_1 . Complications associated with demagnetization effects in the transverse-field experiment and with differences in the superposition of H and H_1 again make quantitative comparisons to the longitudinal-field experiment difficult. On the other hand, the unexpectedly large qualitative differences between $X(H)$ in longitudinal and transverse H demand attention.

The discussion of the demagnetization effects in connection with R in transverse H is equally applicable to $X(H)$. The observed averages of X and Ξ are denoted by \bar{X} and Ξ_{av} . The quantity associated with a unique value of transverse H is designated by Ξ' .

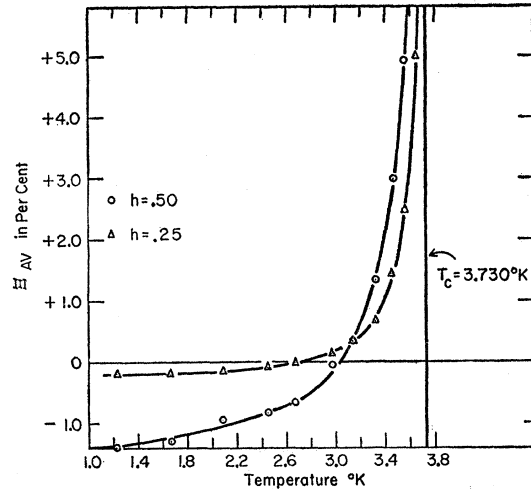


FIG. 16. Relative variation with T of \bar{X} at 1 kMc/sec in superconducting Sn (Sn1) at constant transverse h . The curves $h=0.25$ and $h=0.50$ both correspond to a field dependence of Ξ_{av} more complicated than simple quadratic.

On the other hand, differences in the dynamic superposition of H and H_1 for transverse and longitudinal H affect $X(H)$ and $R(H)$ unequally. Crystalline anisotropy and electronic relaxation effects also complicate the relation between Ξ' and Ξ . In Sec. VI, an estimate is made for (Ξ'/Ξ) on the basis of a two-fluid model applied to the field superposition argument of Ginsburg and Landau.

Results for the temperature dependence of Ξ_{av} at 1 kMc/sec in constant transverse h are presented for Sn1 in Fig. 16. Typical field plots relating to these curves have been presented previously.¹² Because of hysteresis effects occurring at higher h , data are presented for applied $h \lesssim 0.6$.

The characteristics (1), (2), and (3) of Sec. III C are also applicable for comparing $X(H)$ in longitudinal and transverse fields, with the appropriate transcription $R \rightarrow X$. However, there are two important and unexpected differences between the field variation of R and X . One involves the temperature range for which the anomalous decrease in R and in X occurs, and the other concerns differences in the functional form of the field dependence.

Although the anomalous effect in R is absent for Sn1 in transverse H with $T \lesssim 3.3^\circ\text{K}$, the corresponding effect in X persists for T at least as low as 2.1°K . These results need not be considered in contradiction with the Kramers-Kronig relation, but merely imply that there exist frequencies at which the anomalous behavior in X . Such a case was, for example, found by Pippard at 9.4 kMc/sec in transverse h , $3^\circ\text{K} \lesssim T \lesssim 3.63^\circ\text{K}$. Opposite signs for $[R(h) - R(0)]$ and $[X(h) - X(0)]$ at constant T have also been observed at 1 kMc/sec for Sn2 and Sn3 in transverse h and for Sn3 in longitudinal h . The detailed manifestation of this effect depends on

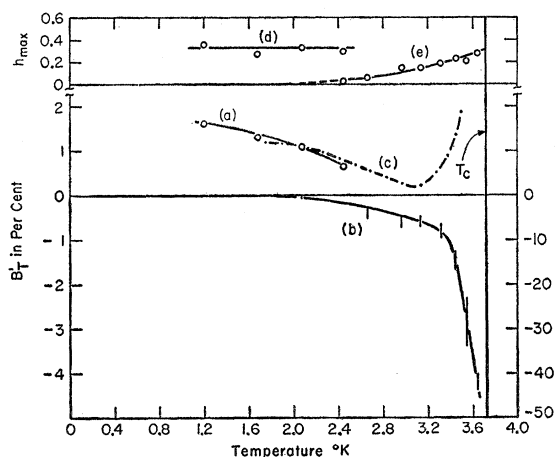


FIG. 17. Lower curves: temperature dependence of the quadratic coefficient, B_T' , of $-\Xi'$ at 1 kMc/sec in transverse h (solid curve). Different T dependences characterize the two branches of B_T' . Curve (a) (branch $B_T' > 0$), following the left-hand scale of ordinates, is determined from the data on Sn1 for $1.2^\circ\text{K} \lesssim T \lesssim 2.5^\circ\text{K}$. Curve (b) (branch $B_T' < 0$), following the right-hand scale of ordinates, corresponds to the anomalous decrease in X with h . The dotted-dash curve (c) illustrates the T dependence of B_T' at 9.4 kMc/sec (Pippard⁵), following the left-hand scale of ordinates (see text). Upper curves: T dependence of h_{max} . Curve (d) corresponds to B_T' in curve (a) and curve (e) to B_T' in curve (b).

crystalline orientation and on the relative direction of H and H_1 .

The functional form of Ξ_{Av} is generally more complicated than of the corresponding Ω_{Av} . There is no accessible range of T for which a quadratic approximation satisfactorily describes Ξ_{Av} (or Ξ') for Sn1 in transverse H . Nevertheless, there are some quadratic aspects of Ξ_{Av} . For T sufficiently low so that the anomalous behavior in X is suppressed, or sufficiently high so it is dominant, the quadratic approximation for Ξ_{Av} is applicable with $h_{\text{max}} \approx 0.3$. For intermediate T , the field dependence of Ξ_{Av} lacks this simplicity. In the normal state $\Xi_{Av} = -1$. Thus, if $\Xi_{Av} > 0$ for some range of h (corresponding to the anomalous effect in X), there must exist a value of h , h_0 , for which Ξ_{Av} is a maximum. As T decreases, the magnitude of both h_0 and $\Xi_{Av}(h_0)$ decreases. Since the functional form of Ξ_{Av} is complicated by the presence of these maxima, the parameters $h=0.25$ and $h=0.50$ of the temperature plots of Fig. 16 cannot be associated with either a quadratic or a nonquadratic field dependence. Furthermore, the curves of Ξ_{Av} vs T (Fig. 16) differ from the corresponding plots in the other three experiments, since Ξ_{Av} in transverse h shows no extrema as a function of T .

Although the functional form of Ξ_{Av} is complicated, the quadratic approximation for transverse h can be applied to analyze the temperature dependence of both the anomalous and low-temperature phenomena. Thus, a comparison can be made with the other three experiments at 1 kMc/sec and with X in transverse h at 9.4

kMc/sec. In Fig. 17, is illustrated the T dependence of the quadratic coefficient of $(-\Xi')$, B_T' , and of the corresponding region of validity of the approximation, $h < h_{\text{max}}$. The effect of demagnetization is taken into account by applying the London equations to an isotropic medium to obtain $B_T' = \frac{1}{2}\bar{B}_T$, where \bar{B}_T is the quadratic coefficient of Ξ_{Av} . The two branches of B_T' are related to the two mechanisms operative on $X(H)$: curve (a) to $X(H)$ increasing monotonically with H , and curve (b) to the anomalous decrease in $X(H)$. [Note that the scale for (b) is a factor 10 greater than that for (a).] Curve (a) is not determined for $T > 2.5^\circ\text{K}$, since the anomalous behavior is too large to permit the two mechanisms to be isolated. In fact, for $T < 2.5^\circ\text{K}$, the persistence of the anomalous decrease in X introduces a systematic error in the determination of the branch $B_T' > 0$, the apparent lowering of curve (a) being accentuated with increasing T . Plots of h_{max} corresponding to (a) and (b) are given by curves (d) and (e), respectively.

A comparison between X in transverse h at 1 and at 9.4 kMc/sec is possible only for the mechanism causing $B_T' > 0$. For this purpose, the dotted-dash curve (c) for B_T' at 9.4 kMc/sec is included in Fig. 17. Curve (c) is obtained from Pippard's data⁵ on $[\lambda(H_c) - \lambda(0)]/\lambda(0)$ (or equivalently on $[X'(h) - X(0)]/[X(0)h^2]$) through (1) multiplication by the T -dependent term, $[X(0)/\Delta X]$ for Sn1 at 1 kMc/sec, and (2) dilation of the scale to obtain a fit with curve (a) at 2.0°K . Although Pippard's measurements do not extend below $T = 1.7^\circ\text{K}$ and curve (a) is confined to $T < 2.5^\circ\text{K}$, it is significant that the two curves show a similar T dependence. Since the systematic error in curve (a) tends to emphasize the decrease in B_T' with increasing T , it is expected that the T dependence of B_T' at 1 and at 9.4 kMc/sec is yet more similar than is seen by comparing curves (a) and (c). The change in scale by a factor 2.0 might be attributed to differences in frequency and in crystalline orientation. The salient feature is that curves (a) and (c) both yield $(\partial B_T'/\partial T)_h < 0$ down to the lowest accessible temperatures. The disagreement between this result and the corresponding behavior in longitudinal h demands attention.

In contrast with the crystalline orientation dependence observed in the other three experiments, Ξ_{Av} in transverse H shows a similar anomalous behavior for all three samples at $t = 0.951 \pm 0.001$ as is seen in Fig. 18. The quantitative dependence of Ξ_{Av} on crystalline orientation (and, perhaps, also on sample purity) is sensitive to temperature.

On the basis of these three orientations, there is insufficient evidence to conclude that $\Xi_{Av} > 0$ always occurs in transverse H . In a preliminary investigation on the indium sample $\alpha = 0.5^\circ$, $\beta = \text{unspecified}$, no anomalous decrease in X was found in transverse H , although a small anomalous effect occurred in longitudinal H .

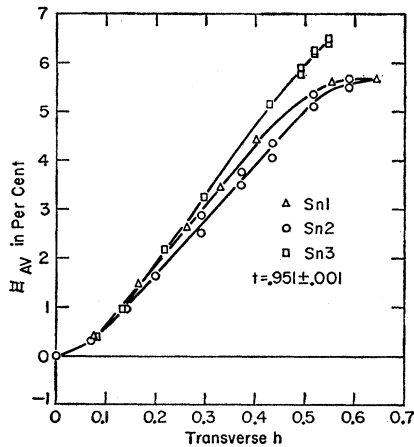


FIG. 18. Relative variation of \bar{X} at 1 kMc/sec with transverse h for three Sn samples (crystalline orientations give in Table I).

V. ERRORS

Although the experimental method is sufficiently sensitive to observe the small changes in the resonance line associated with H , systematic errors limit the accuracy of the experiment. It is felt that these errors affect the quantitative aspects of the problem, but not those qualitative characteristics which have been emphasized, particularly the sign of Ω and Ξ . The maximum resolution of the experiment, corresponding to $\Delta\lambda \approx 0.2$ Å, was attained at low T .

Systematic errors connected with the samples involve the effect of impurities, strain, and imperfect surface conditions. Efforts were made to minimize these errors. Evidence that the samples were adequate to yield meaningful results is provided by agreement with previous results on R and X for $H=0$, metallurgical experience from previous investigations,^{7,10} low surface resistance in the superconducting state at 1.2°K for $H \geq 0$, reproducibility of results on a given sample from one run to another, and reproducibility of results after annealing out cold work (on Sn2). Since the effect of bulk purity on Ω and Ξ was not studied in detail, it is not known whether Sn1 and Sn2 are commensurate with Sn3.

A particularly serious systematic error could result if the application of h to superconducting material could produce normal inclusions. The microwave experiments on R in the limit of low T indicate that the observed changes in $Z(h)$ are connected with the superconducting state, since $(\partial A_L/\partial T)_h$ and $(\partial A_{T'}/\partial T)_h$ are both >0 , and since A_L and $A_{T'}$ become very small in this limit of T . The formation of normal material would depend on h , but not on T .

Errors associated with the microwave technique involve distortions in the resonance line due to frequency-dependent fluctuations in T , H , and in the power level of the resonator. By limiting the input power, distortions caused by H_1 and by the microwave heating of the sample could be adequately reduced,

but with increasing difficulty for $0.96 < t < 1.00$. The strongly attenuating cable leading to the resonator sufficiently decreased the effect of frequency-dependent reflections associated with the coupling mismatch.

Geometrical misalignment of the sample in the resonator could lead to systematic errors depending on the sensitivity of the results to small differences in the direction between H and H_1 . For example, supposing that the anomalous behavior in R and X could only occur in transverse H , then a small tilt of the sample could yield an apparent anomalous behavior in longitudinal H . The experimental design limits the geometrical misalignments to $<2^\circ$ tilt and to <1 mm off-axis (radius of outer conductor in resonator = 1.9 cm). Evidence that the actual misalignments do not invalidate the measurements depends on the reproducibility of the results (1) from run to run, and (2) from different mountings of a given sample in either the same or in different sample holders.

Measurements of Ξ can be made more accurately than of Ω . A small error in the absolute determination of Q_0 at $H=0$ and at $H=H$ could result in a large error in scale factor for Ω , though only affecting the functional behavior slightly. These errors in scale factor are most pronounced at high T because the relative changes in the line widths between $H=0$ and $H=H$ are smallest (see Fig. 6). Larger errors are associated with the measurements in longitudinal h than in transverse h . First of all, the effect of the static field is generally smaller in longitudinal h so that greater sensitivity is needed for its detection. Additional errors in the longitudinal- h experiments are introduced by the small mechanical vibrations resulting from the bubbling of the liquid nitrogen refrigerant for the solenoid. For these reasons, the largest errors are encountered for R in longitudinal h and the smallest for X in transverse h .

VI. DISCUSSION

The results of these four related experiments show that there are two classes of phenomena affecting the surface impedance at 1 kMc/sec of a superconductor in a static magnetic field.

One class deals with the "anomalous" behaviors in R and in X and the relationship between the two. R and X may each decrease with increasing H and a decreasing R need not accompany a decreasing X . By changing the crystalline orientation or the relative direction of H to H_1 , these anomalous effects can be made to vanish. These effects predominate at high T and are strongly dependent on T (and probably also on ν). At least for small h , the field variation of R and X is quadratic for the anomalous behaviors. At present, it is not known whether these phenomena are characteristic of the superconducting electrons, themselves, or of the normal electron current, which is modified by the presence of the superconducting electrons. Although these anomalous behaviors tend to be

emphasized in transverse H , it is felt that sufficient evidence is available to support their occurrence in longitudinal H , also.

The second class of phenomena deals with the low-temperature effects which are relatively insensitive to ν . Theoretical interest is focussed on the functional dependence of $R(h, T)$ and $X(h, T)$ in the limit of low T , since the perturbation of the electron assembly by the static field is least difficult to treat when the electrons are almost entirely in the ground state.

Characteristic of the low-temperature phenomena is the monotonic increase of R and X with h , and the weak field dependence of R and X . The available data suggest that the functional form of $R(h, T)$ and $X(h, T)$ is more complicated than was anticipated. For example, $[R(h) - R(0)]$ cannot be described satisfactorily by only a quadratic term in h in the limit of $T \rightarrow 0$; and the field variation of X is yet more involved. For the crystalline orientation of Sn1, the quadratic coefficient of $[X(h) - X(0)]$ is found to decrease with decreasing T for $1.2^\circ\text{K} < T < 2.0^\circ\text{K}$, while the corresponding coefficient in transverse h increases. Furthermore, it would not be inconsistent with the longitudinal-field data to have the quadratic coefficient of $X(h)$ approach zero as $T \rightarrow 0$. Also of interest is the observation that as T increases, the quadratic approximation for longitudinal h becomes more applicable.

From the point of view of the static field, this presentation has been limited to two principal directions, longitudinal and transverse to the rf current. Because of the large number of variables already present, it is not felt that a discussion of H arbitrarily oriented with respect to H_1 is appropriate at this time. It is believed that the longitudinal- h experiment is the clean-cut, quantitatively significant case. Although previous studies were carried out in the transverse field,⁵ future experiments are likely to emphasize the longitudinal field because of the absence of demagnetization and electronic relaxation effects.

On the other hand, the transverse-field experiments are of qualitative value with regard to both anomalous and low-temperature behaviors. It is likely that the change in both sign and magnitude of Ω and Ξ upon varying H from longitudinal to transverse is connected with the dynamics of the anomalous effects. Also significant is the difference in the crystalline orientation dependence of $R(H)$ and $X(H)$ in transverse and longitudinal H . The transverse-field experiments have also served as a guide to finding the anomalous effects in longitudinal H . Furthermore, the work of Ginsburg and Landau⁹ suggested that by studying the field variation of Z for different directions of H , information could be obtained on the time required to establish equilibrium between the electrons and the rf field.

The Ginsburg-Landau argument⁹ emphasizes the difference in the observation of $Z(H)$ according to whether H is parallel or perpendicular to H_1 . The resonator technique directly examines the rf flux

changes, $\Delta\phi$, which occur in the skin layer of the superconductor as H is applied. In longitudinal H for $|H| \gg |H_1|$ [see Fig. 4(b)], $\Delta\phi$ is caused only by the field variation of the penetration depth, λ . Thus, the field variation of Z and of λ are directly observed in the longitudinal-field experiment. If, however, the electrons can follow the rf field, then the field modulation in transverse H [see Fig. 4(c)] also contributes to $\Delta\phi$, through the time variation of λ . Thus, the measurements in transverse H yield an apparent field variation for Z which is too large by an amount dependent on the relaxation time, τ .

An approximate relation between the transverse- and longitudinal- H experiments can be obtained on the basis of the London two-fluid model, assuming that the electrons follow the rf fields exactly. Suppose that corrections for demagnetization have been applied to the observed λ , R , and X in transverse H to yield $\lambda_{T'}$, $R_{T'}$, and $X_{T'}$. (Denote the corresponding variables in longitudinal H by the subscript L .) By assuming, further, an isotropic medium and a quadratic field dependence for λ , the Ginsburg-Landau argument gives⁹

$$\begin{aligned}\lambda_L &= \lambda^0(1 + \epsilon H^2), \\ \lambda_{T'} &= \lambda^0(1 + 3\epsilon H^2),\end{aligned}\quad (1)$$

where $\lambda^0 = \lambda(H=0)$ [not to be confused with $\lambda_0 = \lambda(T=0)$]. According to the London model for a superconductor with $H=0$, the surface impedance, Z , is connected to λ by^{1,10}

$$Z = R + iX = 4\sqrt{2}\pi^2 i \nu \lambda \mu^{-1} [(\mu+1)^{\frac{1}{2}} - i(\mu-1)^{\frac{1}{2}}], \quad (2)$$

in which

$$\mu = (1 + 4\lambda^4/\delta'^4)^{\frac{1}{2}},$$

and δ' is the classical skin depth appropriate to the normal electron concentration, n_N . As the normal state is approached, n_N increases to n while δ' decreases to a value denoted by δ . Over almost the entire temperature range (e.g., $t < 0.9$), $\mu \ll 1$. Therefore, Eq. (2) can be approximated by

$$\begin{aligned}X &\simeq 8\pi\nu\lambda, \\ R/R_N &\simeq 2\lambda^3/(\delta\delta'^2).\end{aligned}\quad (3)$$

By combining Eq. (1) and Eq. (3), a relation between Ξ_L and $\Xi_{T'}$ follows immediately as

$$\begin{aligned}-\Xi_L &= B_L H^2, \\ -\Xi_{T'} &= B_{T'} H^2 = 3B_L H^2,\end{aligned}\quad (4)$$

where $B_L = \epsilon X(0, T)/\Delta X$. However, the corresponding relation for Ω depends on the field variation of n_N and, therefore, also of δ' . If, in the London model, (n_N/n) is interpreted as $(1 - n_S/n)$, n_S being the superconducting electron concentration, with $(n_S/n) = (\lambda_0/\lambda)^2$, then¹⁸

¹⁸ D. Shoenberg, *Superconductivity* (Cambridge University Press, Cambridge, 1952), second edition, Chap. 6.

$$\begin{aligned}\Omega_L &= A_L H^2, \\ \Omega_{T'} &= A_{T'} H^2 = 3A_L H^2,\end{aligned}\quad (5)$$

with

$$A_L = \{R(0, T)/R_N\} \{3\epsilon + 2[n_S/n_N][\epsilon(T) - \epsilon(0)]\}.$$

It should be observed that since $R(0, T) \rightarrow 0$ as $T \rightarrow 0$, Eq. (5) implies that also $A_L \rightarrow 0$ as $T \rightarrow 0$.

Since A_L and B_L are different functions of ϵ , electronic relaxation affects R and X unequally. Thus, a different T dependence for A_L and B_L can be expected. Furthermore, a more quantitative comparison between the longitudinal- and transverse-field experiments would probably yield $(A_{T'}/A_L)$ and $(B_{T'}/B_L)$ differing from one another and from the value 3. It should be emphasized that the extension of the London theory for $\vec{H}=0$ to relate R and X to λ in the presence of H is not justified. This model is used in the same spirit of approximation as the use of the London equations to correct for demagnetization or as the neglect of crystalline anisotropy effects.

Since the anomalous behaviors in R and X are also strongly dependent on the relative orientations of H and H_1 , this discussion on the dc and rf field superposition is only applicable to the experimental results at low T . At 1 kMc/sec, the observed ratios $(A_{T'}/A_L)$ and $(B_{T'}/B_L)$ are generally greater than the estimated value of 3, ranging up to about 7. However, if ν were too high for the electrons to follow the rf fields exactly, then the Ginsburg-Landau argument could give values < 3 for these ratios; i.e., $1 < (A_{T'}/A_L)$, $(B_{T'}/B_L) < 3$, where the value 1 corresponds to the electrons not following the rf fields at all.

There are yet other differences between the four quadratic coefficients and the ratios between them for Sn1 at 1 kMc/sec.

(1) For $R(H)$ there is a temperature range, $2.5^\circ\text{K} \lesssim T \lesssim 3.3^\circ\text{K}$, in which A_L and $A_{T'}$ are relatively insensitive to T . However, for $T < 2.0^\circ\text{K}$, both A_L and $A_{T'}$ decrease as T decreases, with $(dA_{T'}/dT) > (dA_L/dT)$.

(2) For the temperature-insensitive region, $(A_{T'}/A_L) = 6.7 \pm 1.0$, which exceeds 3. However, for $T \lesssim 2.0^\circ\text{K}$, $(A_{T'}/A_L)$ diminishes with decreasing T , reaching a value of ≈ 2 at $T = 1.2^\circ\text{K}$, suggesting that relaxation by the electrons may become less important for R at low T .

(3) For $X(H)$, $(dB_{T'}/dT)$ and (dB_L/dT) have opposite signs in the range of T , $1.2^\circ\text{K} \lesssim T \lesssim 2.4^\circ\text{K}$, for which the positive branch of $B_{T'}$ can be evaluated. (See Figs. 14 and 17.) The result (3) for X is opposite to that given in (1) for R .

(4) For $1.2^\circ\text{K} \lesssim T \lesssim 2.4^\circ\text{K}$, $(B_{T'}/B_L)$ is increasing with decreasing T , while $(A_{T'}/A_L)$ is decreasing. An order of magnitude estimate for $(B_{T'}/B_L)$ is found from $(B_{T'}/B_L) = 5.0 \pm 0.7$ at $T = 1.2^\circ\text{K}$, which again is larger than 3. The magnitude of $(B_{T'}/B_L)$ appears dependent

on crystalline orientation. That $(B_{T'}/B_L)$ is increasing with decreasing T might suggest that relaxation effects for X become more important at low T in contrast with the results on R .

The available information is insufficient to speculate whether the opposite signs between $(dB_{T'}/dT)$ and (dB_L/dT) and between $[d(B_{T'}/B_L)/dT]$ and $[d(A_{T'}/A_L)/dT]$ persists at still lower temperatures. It is likely that factors other than electronic relaxation are needed to account for the different T dependence of the four quadratic coefficients.

The experiments at 1 kMc/sec differ from Pippard's work at 9.4 kMc/sec in several essential ways. At the higher frequency, measurements were made only in transverse H and on tin samples of unknown crystalline orientation and grain size. The anomalous behavior was reported for R only, although no detailed account of the variation of Ω with h and T was presented. The available data suggest that the anomalous behavior in R persists down to lower T at 9.4 kMc/sec than at 1 kMc/sec, although the magnitude of the effect tends to be larger at the lower ν . On the other hand, if an anomalous behavior in X is present at 9.4 kMc/sec, it is of much smaller magnitude than at 1 kMc/sec. These remarks constitute evidence for the dependence of the anomalous effects on ν . In this connection, it is noteworthy that the occurrence of these effects is associated with (δ_N/λ) having a magnitude of order unity, where δ_N is the rf skin depth for the normal electrons with a concentration n_N in the limit of the extreme anomalous skin effect. At 9.4 kMc/sec, the anomalous behavior in R corresponds to $2.2 \lesssim (\delta_N/\lambda) \lesssim 2.5$, compared with $(\delta_N/\lambda) \lesssim 4.2$ at 1 kMc/sec; the anomalous behavior in X occurs for $(\delta_N/\lambda) \lesssim 6.6$.

At present no quantitative discussion of the ν dependence of the low T effects can be given because longitudinal field data are available only at 1 kMc/sec. However, a qualitative comparison between the transverse-field experiment on X is possible for $1.2^\circ\text{K} \lesssim T \lesssim 2.4^\circ\text{K}$ as is illustrated by the curves (a) and (c) of Fig. 17. Curve (c) is obtained by transforming Pippard's plot⁵ of $(\Delta\lambda/\lambda) \equiv [\lambda(H_c) - \lambda(0)]/\lambda(0)$ vs T to a plot of $\Xi'(H_c^-)$ vs T , using a value of ΔX appropriate to Sn1 at 1 kMc/sec. At 9.4 kMc/sec the variation of X with transverse H can be expressed as a quadratic function of H , for all T with $h \geq 0.5$; however, at the lower ν , the quadratic approximation is only applicable for $h \lesssim 0.32$ [see curve (d)]. On the other hand, the quadratic coefficients, $B_{T'}$, at the two frequencies [curves (a) and (c)] exhibit a similar T dependence, differing by only a scale factor [i.e., $B_{T'}(\nu=1 \text{ kMc/sec})/B_{T'}(\nu=9.4 \text{ kMc/sec}) = 2.0$]. The effects of electronic relaxation, demagnetization and crystalline anisotropy could account for a difference in scale of this magnitude without requiring that the field variation of λ be dependent on ν for this range of ν .

Although the effect of a longitudinal H was not studied in detail at 9.4 kMc/sec, Pippard reported no

detectable difference in $(\Delta\lambda/\lambda)$ between the two principal directions of H .^{1,5} If the electrons do not establish equilibrium with the radiation field, then a meaningful comparison can be made between Pippard's results in transverse H and experiments at 1 kMc/sec in an arbitrarily oriented static field. A comparison with the longitudinal H dependence of Ξ for Sn1 leads to large qualitative differences over the entire range of T , and, in particular, over the region of T , $1.2^\circ\text{K} \lesssim T \lesssim 2.4^\circ\text{K}$, for which qualitative agreement is obtained between the transverse- H studies on X . It is surprising that the functional dependence of B_L is highly sensitive to ν , while B_T' is relatively independent of ν . Since the field variation of λ is more closely connected to the longitudinal- H experiment, it would be reasonable to expect that if any B coefficient is frequency dependent, it would be B_T' rather than B_L . This discussion of the results at the two frequencies indicates the need for further experimental work to establish the functional form of Ξ at low T , with particular emphasis on longitudinal H .

The phenomenological treatment of a superconductor in a magnetic field due to Pippard,⁵ though qualitatively successful in explaining the results at 9.4 kMc/sec near T_c , does not fit the data at the lower ν . Into the Gorter-Casimir two-fluid model is introduced a coherence distance, a , over which no spacial variation of the order parameter, ω , is allowed. The application of the equilibrium condition to the Gibbs free energy, G ,

$$G = -\frac{aH_c^2}{8\pi}[\omega + 2t^2(1-\omega)^{\frac{3}{2}}] - \frac{\lambda H^2}{8\pi}, \quad (6)$$

yields a field-dependent order parameter, $\omega(h)$, determined by

$$0 = 1 - \left\{ \frac{[1-\omega(0)]}{[1-\omega(h)]} \right\}^{\frac{2}{3}} - \frac{[\lambda(0)h^2]}{2a[\omega(h)]^{\frac{3}{2}}}, \quad (7)$$

where $\lambda(0)$ and $\omega(0)$ refer to $h=0$. Physical solutions to Eq. (7) exist only for $\lambda(h) \geq \lambda(0)$, at constant t , with the equality sign corresponding to an infinite coherence distance. Thus, this model does not apply to the anomalous behaviors in R and X . This result is not surprising since the free energy does not explicitly take account of the rf fields, G being independent of ν . It is more unexpected that the model does not seem to apply to Sn1 in longitudinal H , for which $\lambda(h) > \lambda(0)$; i.e., the measurement of Z in longitudinal H shows a decreasing field dependence as $T \rightarrow T_c$, while Eq. (7)

predicts an increased field variation in this limit. It is felt that the high- T phenomena at 1 kMc/sec involve transport processes which must be considered in detail. Perhaps, for ν sufficiently high so that the electrons cannot follow the rf field, ν becomes unimportant and the static model given by Pippard again becomes applicable.

Bardeen's phenomenological treatment,⁶ which was qualitatively successful in explaining the low- T results at 9.4 kMc/sec, also does not seem to apply in its present form to the data at the lower frequency. This model assumes that the superconducting electron wave functions, themselves, are changed by the field. The smallness of the field dependence of λ at 9.4 kMc/sec suggested to Bardeen the use of perturbation theory. Second-order perturbation theory is sufficient to give quadratic terms in the field variation of λ .

The experimental picture at 1 kMc/sec suggests that changes be made in the assumptions put into a low-temperature theory. First of all, the quadratic coefficient of Ξ for Sn1 in longitudinal H decreases with decreasing T , $T \lesssim 2.0^\circ\text{K}$, and the quadratic approximation, itself, becomes less valid in this limit. Secondly, it is not clear that the effect of H is small. Although Ω becomes very small as T decreases below 2.0°K (see Figs. 6, 7, 10), it is worth emphasizing that $[R(H) - R(0)]/R(0)$ is not at all small compared with unity. For example, the quadratic coefficient A_L for Sn1 at 1.2°K is $\approx 0.12\%$ representing an increase in R of about a factor of 2 over $R(0)$. From this point of view, the application of perturbation theory must be made with caution.

The need for further clarification of the experimental situation is indicated. To study the anomalous effects in R and X , it is suggested that emphasis be placed on the ν dependence of Ω and Ξ . Investigations on other crystalline orientations would be fruitful with particular emphasis on simple crystal orientations such as (1) $\alpha=0^\circ$, (2) $\alpha=90^\circ$, $\beta=0^\circ$, (3) $\alpha=90^\circ$, $\beta=45^\circ$. The effect of the addition of small amounts of impurities on the anomalous behavior of R and X may prove significant. Systematic studies are needed to establish the functional form of Ω and Ξ in the limit of low T .

ACKNOWLEDGMENTS

The author wishes to express her gratitude to Dr. A. B. Pippard for direction during the initial stages of this work and for many valuable suggestions and to Professor A. W. Lawson and Professor E. A. Long for their continued interest and encouragement.